ADVANCED FUNCTIONAL MATERIALS
www.afm-journal.de

www.MaterialsViews.com

# Controlling the Chromaticity of Small-Molecule Light-Emitting Electrochemical Cells Based on TIPS-Pentacene

*Michael D. Weber, Matthias Adam, Rik R. Tykwinski, and Rubén D. Costa**

**This work demonstrates a novel proof-of-concept to implement pentacene derivatives as emitters for the third generation of light-emitting electrochemical cells based on small-molecules (SM-LECs). Here, a straightforward procedure is shown to control the chromaticity of pentacene-based lighting devices by means of a photoinduced cycloaddition process of the 6,13-bis (triisopropylsilylethynyl) (TIPS)-pentacene that leads to the formation of anthracene-core dimeric species featuring a high-energy emission. Without using the procedure, SM-LECs featuring deep-red emission with Commission Internationale d'Eclairage (CIE) coordinates of $x = 0.69/y = 0.31$ and irradiance of 0.4 μW cm$^{-2}$ are achieved. After a careful optimization of the cycloaddition process, warm white devices with CIE coordinates of $x = 0.36/y = 0.38$ and luminances of 10 cd m$^{-2}$ are realized. Here, the mechanism of the device is explained as a host–guest system, in which the dimeric species acts as the high-energy band gap host and the low-energy bandgap TIPS-pentacene is the guest. To the best of the knowledge, this work shows the first warm white SM-LECs. Since this work is based on the archetypal TIPS-pentacene and the photoinduced cycloaddition process is well-knownfor any pentacenes, this proof-of-concept could open a new way to use these compounds for developing white lighting sources.**

## 1. Introduction

Acenes have attracted a wide interest in both scientific and industrial communities during the last decade.[1–4] They are described as aromatic hydrocarbons that consist of linearly fused benzene rings. As the most outstanding features, the band gap is easily tuned by increasing the number of benzene condensed rings, while the stability and solubility are enhanced by attaching peripheral bulky groups. More relevant is that a proper molecular design leads to significant breakthroughs when they are applied in small-molecule optoelectronic devices, such as organic field effect transistors (OFETs), organic photovoltaics, organic light-emitting diodes (OLEDs), among others.[1–7]

The so-called TIPS-pentacene—6,13-bis(triisopropylsilyleth ynyl)pentacene as shown in **Figure 1**b—has emerged as one of the most intriguing archetypal compounds. For instance, remarkable charge mobilities of up to 4.6 cm$^2$ V$^{-1}$ s$^{-1}$ for its solution-sheared thin films applied in OFETs have been achieved.[8] Recently, the same authors have demonstrated that the control of the structural arrangement in films boosts the field-effect mobility to remarkable values of 11 cm$^2$ V$^{-1}$ s$^{-1}$.[9] In addition, this molecule has recently emerged as a paradigm to study singlet fission process in both solution and thin films, owing to its triplet quantum yield formation exceeding values of 100%.[5,6,10–13] Finally, the sharp red emission at around 650 nm and the moderate photoluminescence quantum yields (PLQYs) when dispersed in a thin film with the electron-transporting host tris(quinoline-8-olato)-aluminum(III) ($Alq_3$) prompted Kafafi and Anthony groups to fabricate the first OLEDs based on trialkylsilylethynyl-substitute pentacenes.[14,15] As the most remarkable result, the authors demonstrated that through a proper design of the molecular structure a near quantitative internal quantum efficiency based on the PLQYs of the active layer is realized.[16] Encouraged by this excellent result, we decided to probe the performance of the archetypal TIPS-pentacene as an emitter in small molecule light-emitting electrochemical cells (SM-LECs).

LECs have emerged as an interesting alternative to OLEDs due to the single-layer device architecture based on air-stable electrodes, the high power efficiencies at very low operation voltages, and the low-cost manufacturing process on any 3D-shaped substrate.[17–22] These assets are possible due to the unique mechanism as the active layer comprises a blend of mobile ions and mostly one electroactive compound.[23–27] Up to date, the most representative materials for LECs have been mixtures of a light-emitting polymer, an ion conducting polymer, and an inorganic salt, as well as mixtures of ionic transition-metal complexes (iTMCs) and ionic liquids.[19–21] However, Edman and co-workers have recently demonstrated that the LEC concept can be easily expanded to small molecule (SM) materials.[28] This result represents a landmark toward future breakthroughs in the field, especially if we take into account the very recent achievements in SM-based OLEDs that are considered as the new momentum heading into the third generation of this technology,[29–33] as well as SMs are considered as the third generation of materials for LECs, which is now in its early infancy.[28,34]

M. D. Weber, M. Adam, Prof. R. R. Tykwinski, Dr. R. D. Costa
Department of Chemistry & Pharmacy
University of Erlangen-Nuremberg
91058 Erlangen, Germany
E-mail: ruben.costa@fau.de

DOI: 10.1002/adfm.201501326

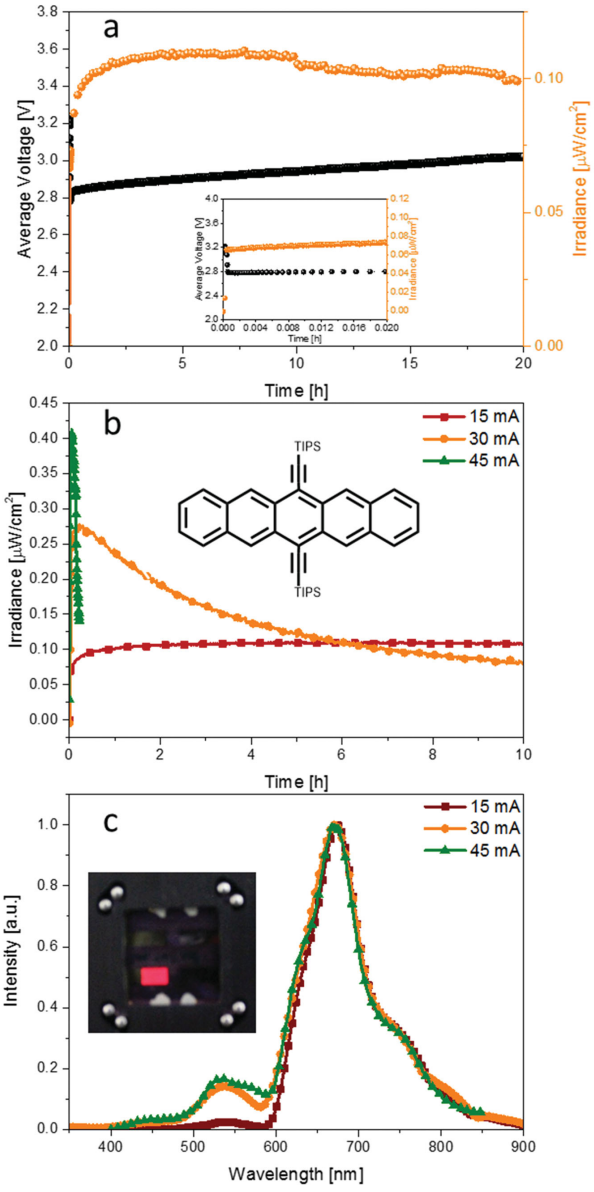


**Figure 1.** a) Average voltage and irradiance values over time of fresh TIPS-pentacene LECs driven at an average pulsed current of 15 mA. The early device response is shown as an inset. b) Irradiance over time of fresh TIPS-pentacene LECs driven at different pulsed average currents. The chemical structure of the TIPS-pentacene is shown as an inset. c) EL spectra of fresh TIPS-pentacene LECs driven at different pulsed currents at the earlier moments of the device operation. Photograph of the running device is also included as inset.

Herein, we report for the first time on the integration of pentacenes as emitters in the field of SM-LECs, emphasizing the most significant achievements and limitations of this family in ionic-based lighting devices. More importantly, this work provides a proof-of-concept to exploit a unique feature of the pentacene family, that is, the photoinduced cycloaddition process to create high-energy emitting anthracene-core species,[35] providing the first example of white SM-LECs when this process is controlled. To settle a fundamental and novel approach, the archetypal TIPS-pentacene was the molecule of choice—Figure 1b. In detail, while stable deep-red electroluminescence was achieved when the TIPS-pentacene was blended with a standard ionic polyelectrolyte—see the Experimental Section for more details—an unexpected and weak band centered at the high-energy region of the electroluminescence (EL) spectrum was noted. The latter was intriguing enough to keep our attention, since a) it has never been observed before in OLEDs due to the use of the $Alq_3$ host that also emits in this region, and b) the enhancement of this unique electroluminescence feature could be exploited toward the fabrication of the first white SM-LECs. In the work at hand, we demonstrated for the first time that the high-energy band is related to the formation of anthracene-core dimeric species. Here, the mechanism of the device is explained as a host–guest system, in which the dimeric species act as the high-energy band gap host and the low-energy band gap TIPS-pentacene as the guest. More importantly, we demonstrate how to control this process as a new method to easily tune the chromaticity of the devices, realizing deep-red and warm white SM-LECs—Commission Internationale d'Eclairage 1931 (CIE) coordinates of $x = 0.69/y = 0.31$ and $x = 0.36/y = 0.38$, respectively. Overall, this work provides a proof-of-concept that opens a new avenue to fabricate white lighting sources based on pentacene derivatives.

## 2. Results and Discussion

Lighting sources based on LECs with a sandwich-like architecture were our focus of research. The active layer consists of a mixture of the TIPS-pentacene emitter and the ionic polyelectrolyte—i.e, $LiCF_3SO_3$ dissolved in trimethylolpropane ethoxylate (TMPE) with the mass ratio of 0.3:1. The latter is deposited between an indium-tin oxide (ITO) substrate modified with a poly(3,4-ethylenedioxythiophene)polystyrene sulfonate (PEDOT:PSS) layer as anode and a layer of aluminum deposited on top of the active layer as cathode—see the Experimental Section for more details.

Similar to that reported on pentacene-based OLEDs,[4,14] we decided to drive the devices at different applied currents, but using a pulsed driving scheme based on a block-wave at 1000 Hz and a duty cycle of 50%. Notably, this driving mode has led to the best performing LECs in terms of a stable performance and ultrafast turn-on times.[36] Figure 1a shows the average voltage and irradiance for LECs driven under pulsed current conditions. In excellent agreement with the few reports on SM-LECs,[28,34] the device response shows the typical features of ionic-based lighting devices. In particular, the average voltage required to apply different currents is initially high and rapidly reduces over time followed by an increase of the irradiance that reaches its maximum value, featuring extrapolated lifetimes of around 100 h. It should be noted that the relative moderate irradiances are caused by the extremely weak photoluminescence response of the active layers—PLQYs < 0.5% as also observed by other groups.[14,15] To obtain higher irradiances, the applied current was increased. This procedure shows, however, a drawback regarding the device stability—Figure 1b. Regardless of the stability, the best irradiance value is 0.4 μW $cm^{-2}$. Although this value is moderately low for red-emitting LECs, we must consider that no optimization in terms of charge transport

features and suppression of aggregates that act as quenchers have been performed yet.[14,15,37]

More relevant is the analysis of the EL spectra. Upon applying the lowest driving current, deep-red LECs with CIE coordinates of $x = 0.69/y = 0.31$ and EL spectra that consist of a maximum at ≈670 nm and a shoulder at 750 nm were obtained—Figure 1c. At this point, it is important to state four major aspects. First, the EL process arises from a molecular emission that occurs from an electronic excited state similar to that noted for photoluminescence (PL), as the most prominent features at 670 nm in EL versus 650 nm in PL suggest—Figure S1 (Supporting Information). Second, the significant shift of around 50 nm for the low-energy shoulder in the EL compared to the PL strongly suggests the presence of weak emissive aggregates as also noted for pentacene-based OLEDs,[14,15] even though the mixture with the polyelectrolyte was expected to hinder the crystallization of the pentacene during the layer deposition. As aforementioned, this prompts us to suggest that the presence of aggregates is one of the reasons for the moderate irradiance.[14,15] Third, it is important to point out that the shape of the EL spectrum remains unchanged over time—see the 3D plot in Figure S2 (Supporting Information), suggesting that the main reason for the loss in irradiance is the intrinsic device mechanism.[23–27] Finally, it is striking to note a weak and broad band at the high-energy region. This is clearly noted from the early moments of the device response and gains in intensity when the device is driven at high currents—Figure 1c. By contrast, the low-energy region features remain unchanged upon applying different driven currents. Notably, the high-energy band was already observed by Kafafi and Anthony groups in pentacene-based OLEDs and it was judiciously ascribed to the residual emission of the $Alq_3$ host as the energy transfer process was inefficient.[14,15] This explanation is, however, not applicable in our devices, since we do not have any electron transport host matrix and the polyelectrolyte does not show any EL response. As such, this band is best ascribed to a) the degradation of the TIPS-pentacene to high-energy emitting species under operation conditions, b) the formation of aggregates that blue-shift the emission during device operation,[38,39] and/or c) the formation of new species prior to the layer fabrication.

To study the first hypothesis, repetitive current density and irradiance as a function of applied voltage during several scans at $dV/dt = 0.1\ V\ s^{-1}$ were performed—**Figure 2**a,b. No degradation in terms of both current density and irradiance profiles, as well as the shape of the EL spectrum were noted. In addition, the rise and decay times of the bands centered at 540 and 670 nm were fitted by using exponential functions for devices driven at different pulsed currents, inferring different rate constants of both processes for each band—Figure 2c. For instance, the rising constants of the 540 and 670 nm bands were 20.01 and 28.60 $h^{-1}$, as well as 42.20 and 100 $h^{-1}$ for devices driven at 30 and 45 mA, respectively. In the same manner, decay constants of 0.23 and 0.09 $h^{-1}$, as well as 3.70 and 1.56 $h^{-1}$ for 540 and 670 nm bands in devices driven at 30 and 45 mA, respectively, were determined. Since no apparent link is derived between the rising and decay processes and the electronic features of the device remain constant, we can safely rule out that the new band is ascribed to the degradation of the TIPs-pentacene to high-energy emitting species under device

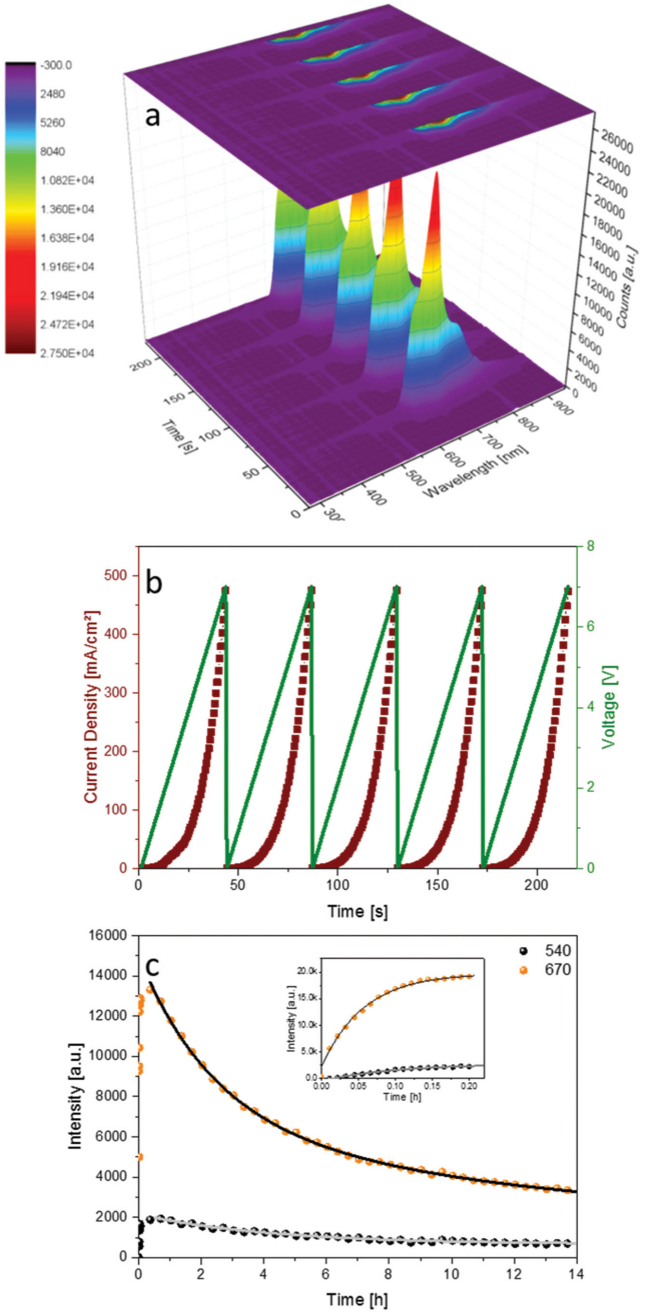


**Figure 2.** a) EL spectra changes of fresh TIPS-pentacene LECs under five cycles of applied voltage. b) Current density and applied voltage profiles of fresh TIPS-pentacene LECs under five cycles of applied voltage. c) Intensity profiles of the EL bands centered at 540 and 670 nm of fresh TIPS-pentacene LECs driven at average pulsed currents of 30 and 45 (inset) mA. The solid lines are the fittings for the decay and the rising (inset) processes.

operation conditions. Likewise, we believe that the formation of aggregates caused by either the distribution of the polyelectrolyte under operation conditions or the high electric field across the thin active layer is unlikely, since the high-energy band appears immediately after switching on the device—Figures 1c and 2c. To further support this notion, we carried out a simple

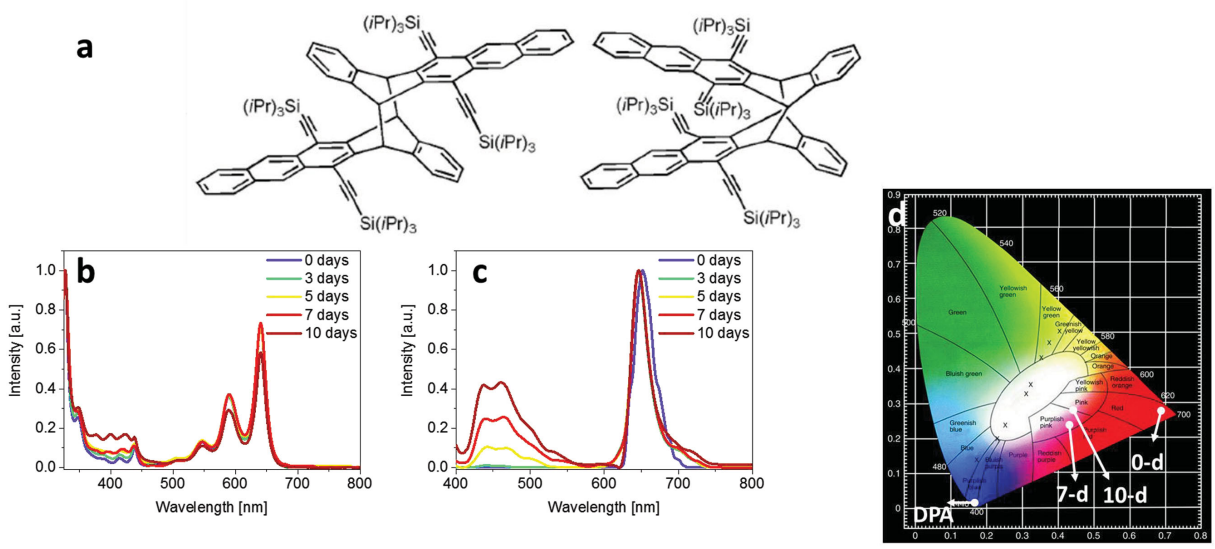


**Figure 3.** Upper part – a) Chemical structures of the anthracene-core species as suggested by Coppo and Yeates.[35] Lower part – b) normalized absorption and c) emission spectra measured over time, as well as d) CIE coordinates of TIPS-pentacene mixed with the ionic polyelectrolyte in solution.

experiment by heating a device at different temperatures. Here, the heating process erases the ion distribution and the p- and n-doped regions and, in turn, it might also destroy the possible aggregates that could be formed under operation conditions. Thus, four devices were driven at an average pulsed current of 15 mA until the brightness started to decay taking the electroluminescence spectra at this point, then they were stopped and placed on a hot plate for 30 min each at 80 and 150 °C under inert atmosphere and ambient light. Following heating, the EL spectrum was recorded when the same steady-state was reached as before the heating process. Noteworthy, the device was destroyed when heating at higher temperatures was attempted, as the changes in the color of the cathode suggested. As shown in Figure S3 (Supporting Information), the averages of the relative intensities between the high- and low-energy bands are independent of the temperature. Thus, this finding confirms that both the degradation of the emitter to high-energy emitting species and the formation of aggregates during operation conditions are not the reasons for the new band at the high-energy regions.

Finally, the possible formation of new species during device fabrication was studied by monitoring the absorption features of the solutions stirred in a sealed vial over time from 0 to 10 d. As shown in **Figure 3**b, the intensity of the absorption bands related to the TIPS-pentacene at

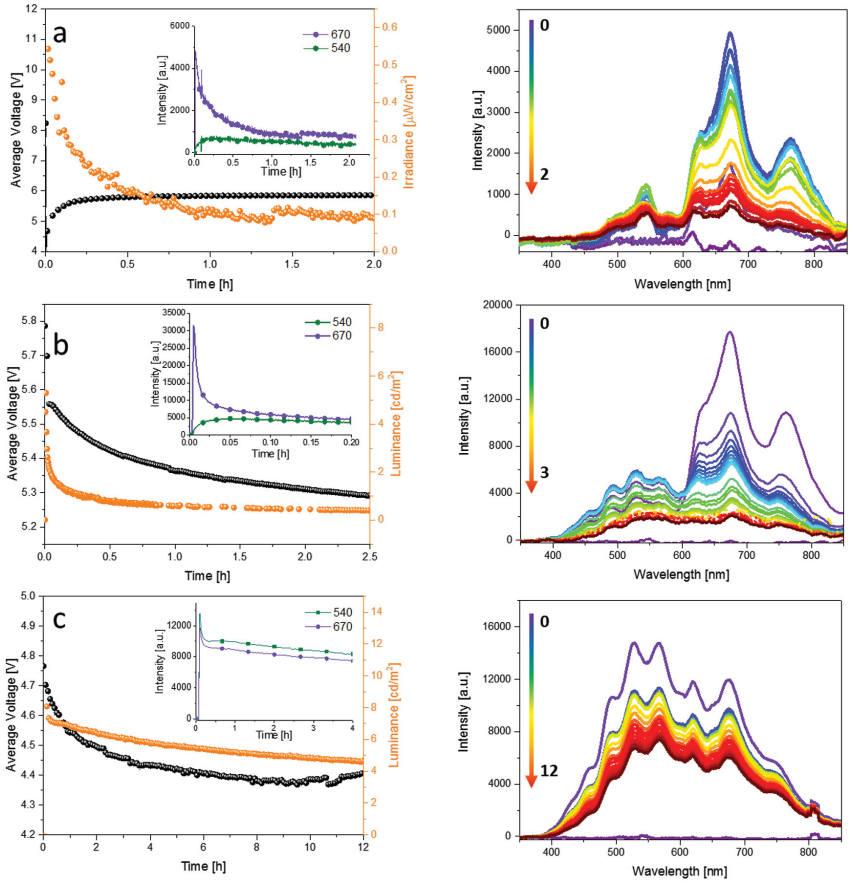


**Figure 4.** From a) to b) and c), the left part displays the average voltage and brightness values over time of 3, 7, and 10 d LECs driven at an average pulsed current of 45 mA, respectively. The insets display the profile of the EL response at both high- and low-energy regions. The right part shows the EL spectra evolution of 3, 7, and 10 d LECs driven at an average pulsed current of 45 mA. The time scale is in hours.

640, 590, and 545 nm slowly decreases along with a simultaneous increase of the bands located at 380, 400, and 425 nm. According to previous work,[35,40] this suggests a photoinduced cycloaddition process that occurs selectively at the 5- and 14-positions, forming a dimer with an anthracene core—the proposed molecular structure of the photodimerized species is shown in Figure 3a. High-resolution mass spectrometry (HRMS) and MS/MS analyses were performed on samples from the fresh and 10 d old solutions, using atmospheric pressure photoionization (APPI) as the ionization method—Figure S4 (Supporting Information). MS analysis indicated the presence of the dimers only in the 10 d old solutions. In detail, a mass signal of m/z = 1277.7568 was found experimentally, consistent with that expected for the protonated dimer ($[M + H]^+$, $C_{88}H_{109}Si_4$, calculated m/z = 1277.7606). While encouraging, the presence of the signal of the dimer at m/z = 1277.8 does not establish the constitution of this species—i.e., does the dimer arise from a supramolecular or a covalently linked species? To shed light onto this question, MS/MS experiments were performed for the 10 d solutions. Focusing on the signal at m/z = 1277.8 as the precursor ion—i.e., the dimer, fragmentation was induced using collision-induced dissociation by nitrogen. A fragment signal at m/z 639.38467 which is consistent with the protonated "monomer"—i.e., TIPS-pentacene, was detected starting at collision energies at 44 eV. The lack of a fragment signal at lower collision energies supports the presence of a covalently bound dimer, rather than a dimer resulting from supramolecular aggregation. Further corroboration is provided by concentration dependence steady-state PL assays—Figure S5.

More interesting is the PL features of the solutions under excitation at 310 nm—Figure 3c. Besides the well-structured emission of the pentacene at 650 and 710 nm, a new broad emission band at the high-energy region evolves. In detail, the intensity and the vibrational structure of the new emission band is enhanced over time, followed by a blue-shift of around 5 nm of the low-energy emission features. Finally, to further support that the nature of the dimers is covalent, we have also monitored the emission features of the aged solution upon dilution from $10^{-4}$ to $10^{-8}$ M, as well as adding a high concentration of a surfactant—i.e., 1000:1 molar ratio chenodeoxycholic acid:TIPS-pentacene—to further break any possible supramolecular aggregates in the $10^{-8}$ M solution—see Figure S5 (Supporting Information). Here, the high-energy emission features are changeless upon both decreasing the concentration and adding the excess of surfactant. With this data at hand, we hypothesize that the high-energy EL emission should be ascribed to dimeric species as proposed by Coppo and Yeates—Figure 3a.[35]

Taking into consideration that the PL of the solutions evolve from deep-red to pinkish-white—the 10 d samples feature a CIE of $x = 0.46/y = 0.28$ as shown in Figure 3d, the question is whether we might use this unique behavior of pentacene to control the chromaticity of the EL response towards white devices. To this end, our first step was to fabricate devices with solutions aged 3, 7, and 10 d. In line with the performance of the fresh device, the 3 d device—i.e., from solution aged 3 d—shows an initial reddish orange color ($x = 0.55/y = 0.40$) caused by the more prominent high-energy band than that of

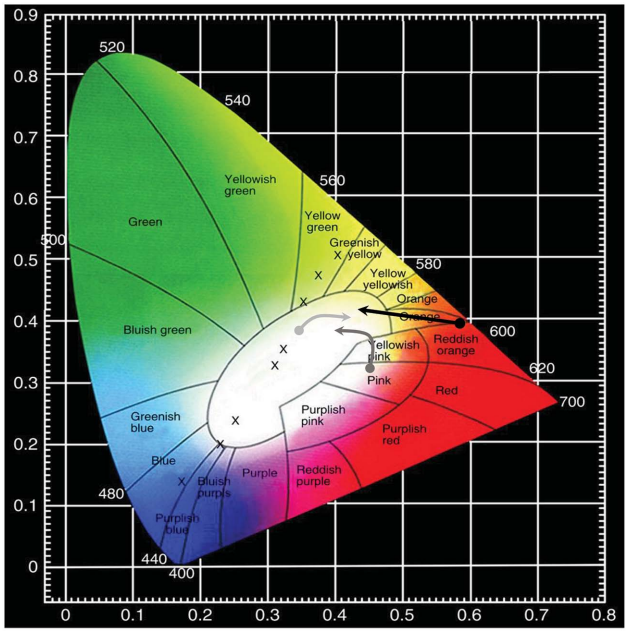


**Figure 5.** Changes of the CIE coordinates over time of 3, 7, and 10 d devices driven at an average pulsed current of 45 mA. Black, dark grey, and light grey lines correspond to 3, 7, and 10 d devices, respectively.

the fresh device—**Figure 4**a. Dependent on the driving current, the intensity of low-energy contribution decreases over different times in the range of hours, achieving a weak yellowish white EL emission ($x = 0.49/y = 0.45$) that holds until the device reaches its lifetime limit—**Figures** 4a and **5**. On the contrary, warm white and much brighter EL is realized from 7 and 10 d devices. For instance, 7 d devices need between a few minutes to less than 0.5 h upon reducing the driving currents to achieve warm white EL ($x = 0.40/y = 0.38$) with moderate luminances of ≈6 cd $m^{-2}$—Figures 4b and 5. The initial high intensity of the red part of the spectrum followed by its fast decay until reaching the same intensity levels as the high-energy features suggest a similar mechanism as in the host–guest approach.[41,42] Owing to the low-energy band gap of TIPS-pentacene compared to the dimeric species, we could consider the TIPS-pentacene as the guest that is diluted into the high band-gap anthracene-core species, or host, upon increasing the time of the cycloaddition process. In this scenario, the energy alignment of the host–guest system disrupts carrier injection and trapping on the TIPS-pentacene as the concentration of the guest is reduced. On one hand, this decreases the rate of carrier recombination and/or exciton formation on the guest, resulting in lower applied voltages to keep the required current, as well as a fast decay of the guest emission contribution as shown in Figure 4. On the other hand, the intensity of the host emission is gradually increased along with its concentration in the active layer. Notably, the same behavior is observed for the guest emission, quite likely owing to the enhancement of the PLQYs upon dilution into the host material until its concentration is significantly reduced in the 10 d devices—Figure 4. It is important to note that, under electrical excitation, the intensity of the high-energy region bands does not increase over time nor new features emerge, but they equal to the low-energy bands decreasing together in

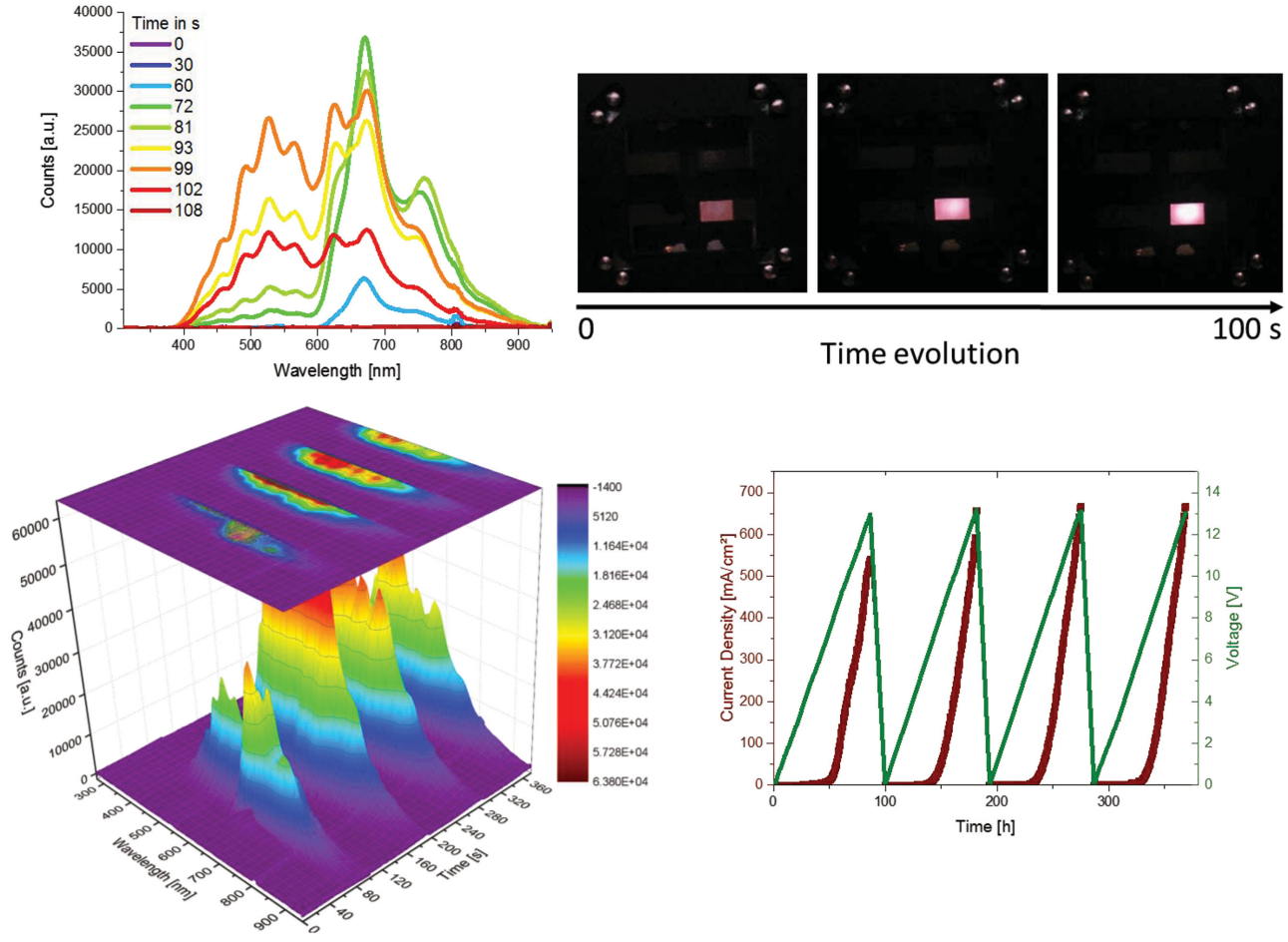


**Figure 6.** Upper part – Changes of the EL spectra from deep-red to white of 7 d LECs under the first cycle of applied voltage. Bottom part – EL spectra (left) and current density and applied voltage profiles (right) of 7 d LECs under five cycles of applied voltage.

intensity—Figure 4. This clearly indicates that there is a lack of degradation of the TIPS-pentacene under electrical conditions as already mentioned in the fresh devices—Figure S2 (Supporting Information). As such, the degradation of the device must be ascribed to its intrinsic mechanism.[23–27]

Next, electrical conditioning schemes were applied to further optimize the EL chromaticity of the 7 d devices. We postulate that the saturation of the initial charge trapping in the TIPS-pentacene is reached by using repetitive voltage cycles, resulting in instantaneous warm white emission. As shown in **Figure 6** and Figure S6 (Supporting Information), during the first cycle the color of the device develops from red to white, which holds during the next five cycles and for a subsequent device operation independent of the driving currents. This clearly supports the aforementioned host–guest hypothesis. Striking enough is that the electrical conditioning is not necessary for 10 d devices as shown in Figure 4c and Figure S7 (Supporting Information). Here, instantaneous and stable warm white devices featuring luminances of ≈10 cd $m^{-2}$ were achieved. Notably, aging more than 10 d leads to devices featuring a yellowish green EL response due to the lack of the guest emission—Figure S8 (Supporting Information). In other words, the 10 d device represents the best balance between instantaneous warm white emission and low applied voltage as shown in Figure 4c. Nevertheless, the limited brightness is to some degree associated with the relatively low photoluminescence of the films—PLQYs < 0.5%. By further improving this family of compounds to provide higher emission efficiencies in thin films, it is believed that the brightness can be much further enhanced in the future.

Finally, we focused on a direct comparison of the 10 d devices with traditional host–guest devices, in which we diluted several amounts of TIPS-pentacene in 9,10-diphenylanthracene (DPA) solutions. The optimized molar ratio of TIPS-pentacene (guest) and DPA (host) in terms of similar EL contributions from both components was 1:99. As shown in **Figure 7**, two major findings are highlighted. On one hand, direct comparison of the EL spectra of fresh and 10 d devices and TIPS-pentacene/DPA devices confirms that the high-energy emission is ascribed to species with an anthracene-core—Figure 7a,b. Indeed, the vibrational progression of the EL spectrum of the 10 d device nicely matches with those resulting from the DPA and TIPS-pentacene EL spectra. On the other hand, our devices outperform in terms of brightness and chromaticity the traditional

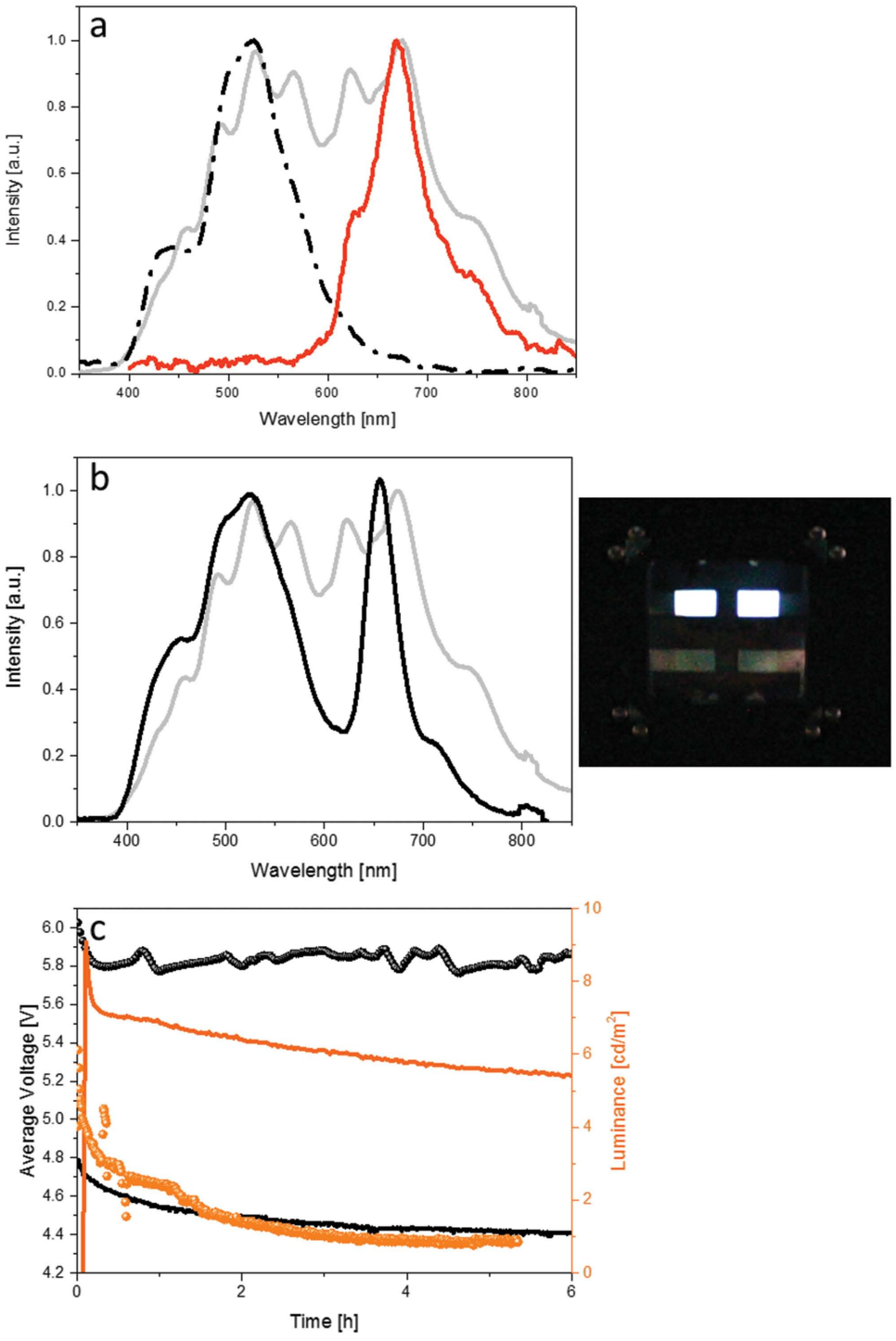


**Figure 7.** a) EL spectra of devices with DPA (dash-doted line), TIPS-pentacene (dark solid line), and 10 d TIPS-pentacene (light solid line). b) EL spectra of 10 d LECs (grey) and DPA/TIPS-pentacene LECs (black) devices driven at an average pulsed current of 45 mA. The right side shows a photograph of a running 10 d LEC. c) Average voltage-brightness profile over time of 10 d (solid line) and DPA/TIPS-pentacene (symbol) devices driven at average pulsed current of 45 mA.

host–guest devices—Figure 7c. For instance, although the EL spectrum of the traditional host–guest device covers the whole visible spectra, the intensity in the middle region is rather low, compromising the color of the device. At the same time, the brightness is slightly lower than in the 10 d device. This is quite likely related to a more prominent charge trapping at the guest units that strongly reduces the exciton recombination rate.[41,42] It should be pointed out that the latter could also be

caused by the aggregation of the DPA and/or phase separation issues between both components. Thus, a better molecular design of the host could outperform the 10 d devices. Besides the latter, the direct comparison of the above described devices doubtlessly confirms that the high-energy band comes from anthracene-core dimeric compounds and that the aging of the pentacene solution is a unique strategy to fabricate white lighting devices.

## 3. Conclusion

In summary, this work demonstrates for the first time a novel proof-of-concept to implement pentacene derivatives as emitters in SM-LECs, showing a straightforward procedure to control the chromaticity of pentacene-based lighting devices by means of a photoinduced cycloaddition process before device fabrication. After a careful optimization of this process, we were able to fabricate the first warm white SM-LECs. Even more relevant, since we have demonstrated it with the archetypal TIPS-pentacene and the photoinduced cycloaddition process is well-known for any pentacene derivative, this approach could be considered as a proof-of-concept that opens a new way to use this family of compounds for developing white lighting sources. Finally, it is important to point out that the most severe limitation is the intrinsic low PLQY of the TIPS-pentacene layers due to the formation of aggregates. This also applies to the host compound, which is also prone to aggregate in solid state. Although the aggregation issue in thin films compromises the device performance, there are well established strategies to modify the molecular structure of both pentacene and anthracene through, for example, the incorporation of sterically demanding groups.[4,14,15] Indeed, several groups have recently focused on modifying different families of acenes with iptycene units to avoid the photoluminescence self-quenching produced in thin-films, showing a significant enhanced performance in OLEDs.[43–45,16] As such, this might be considered as a future strategy to enhance the overall efficiency even more.

## 4. Experimental Section

*Materials*: TIPS-pentacene was prepared following the synthesis reported elsewhere.[46] Other materials like 9,10-diphenylanthracene (DPA), $LiCF_3SO_3$ (≥98%), trimethylolpropane ethoxylate ($M_n \approx 450$ molecular weight), and Tetrahydrofuran (THF) anhydrous (≥99.9%) were purchased from Sigma-Aldrich and used as received. PEDOT:PSS (Clevios P Al4083) were purchased from Heraeus.

*Characterization Techniques*: Steady-state absorption spectra were recorded with a Perkin Elmer Lambda 35. Steady-state emission spectra were recorded with a Fluoromax-P-spectrometer from HORIBA Jobin Yvon. Mass spectra were obtained from Bruker 9.4T Apex-Qe FTICR, Shimadzu AXIMA mConfidence (MALDI-TOF), Bruker micro TOF II, and Bruker maxis 4G (APPI, ESI) instruments.

*Device Fabrication and Characterization*: Double layer LECs were fabricated as follows. ITO coated glass plates were patterned by conventional photolithography (Naranjo Substrates). The substrates were cleaned by using sequential ultrasonic baths, namely, in water–soap, water, ethanol, and propan-2-ol solvents. After drying, the substrates were placed in a UV–ozone cleaner (Jelight 42-220) for 10 min. An 100 nm layer of PEDOT:PSS was doctor-bladed onto the ITO-glass substrate to increase the device preparation yield (400 µm substrate distance and a speed of 10 mm $s^{-1}$). The luminescent layer comprised a mixture of the TIPS-pentacene with $LiCF_3SO_3$ dissolved in TMPE with the mass ratio of 1:0.03:0.1, respectively. The solutions were stirred in a sealed vial over time. The active layer was deposited by means of doctor blading technique (600 µm substrate distance and a speed of 25 mm $s^{-1}$) reaching a thickness of 60 nm. These conditions resulted in homogenous thin films with a roughness less than 5%, having no apparent optical defects. The latter was determined using the profilometer DektakxT from Bruker. Once the active layer was deposited, the samples were transferred into an inert atmosphere glovebox (<0.1 ppm $O_2$ and $H_2O$, Innovative Technology). Aluminum cathode electrode (90 nm) was thermally evaporated using a shadow mask under high vacuum (<1 × $10^{-6}$ mbar) using an Angstrom Covap evaporator integrated into the inert atmosphere glovebox. Up to 16 devices were prepared from aged solutions, that is, fresh, 3, 7, 10, and 15 d old solutions, which were prepared from three different batches of the TIPS-pentacene. Time dependence of luminance, voltage, and current was measured by applying constant and/or pulsed voltage and current by monitoring the desired parameters simultaneously by using Avantes spectrophotometer (Avaspec-ULS2048L-USB2) calibrated with a white LED in conjunction with a sphere Avasphere 30-Irrad and Botest OLT OLED Lifetime-Test System. Electroluminescence spectra were recorded using the above mentioned spectrophotometer.

## Supporting Information

Supporting Information is available from the Wiley Online Library or from the author.

## Acknowledgement

The authors acknowledge funding from the Bavarian Network "Solar Technologies Go Hybrid." This work was also supported by the "Fonds der Chemischen Industrie" (FCI) in the Liebig grant framework and by the EAM Starting Grant of the Cluster of Excellence "Engineering of Advanced Materials" (EAM) promoted by the German Research Foundation (DFG) within the framework of its "Excellence Initiative." Finally, the authors thank the referees for their comments, which have improved to this work and Professor Thomas Drewello for helpful advice regarding the MS/MS experiments.

Received: April 2, 2015
Revised: June 2, 2015
Published online: July 14, 2015

[1] J. E. Anthony, *Nat. Mater.* **2014**, *13*, 773.
[2] Q. Ye, C. Chi, *Chem. Mater.* **2014**, *26*, 4046.
[3] M. Watanabe, K.-Y. Chen, Y. J. Chang, T. J. Chow, *Acc. Chem. Res.* **2013**, *46*, 1606.
[4] J. E. Anthony, *Chem. Rev.* **2006**, *106*, 5028.
[5] J. Lee, P. Jadhav, P. D. Reusswig, S. R. Yost, N. J. Thompson, D. N. Congreve, E. Hontz, T. Van Voorhis, M. Baldo, *Acc. Chem. Res.* **2013**, *46*, 1300.
[6] D. N. Congreve, J. Lee, N. J. Thompson, E. Hontz, S. R. Yost, P. D. Reusswig, M. E. Bahlke, S. Reineke, T. Van Voorhis, M. Baldo, *Science* **2013**, *340*, 334.
[7] H. Dong, X. Fu, J. Liu, Z. Wang, W. Hu, *Adv. Mater.* **2013**, *25*, 6158.
[8] G. Giri, E. Verploegen, S. C. B. Mannsfeld, S. Atahan-Evrenk, D. H. Kim, S. Y. Lee, H. A. Becerril, A. Aspuru-Guzik, M. F. Toney, Z. Bao, *Nature* **2011**, *480*, 504.
[9] Y. Diao, B. C.-K. Tee, G. Giri, J. Xu, D. H. Kim, H. A. Becerril, R. M. Stoltenberg, T. H. Lee, G. Xue, S. C. B. Mannsfeld, Z. Bao, *Nat. Mater.* **2013**, *12*, 665.

[10] B. J. Walker, A. J. Musser, D. Beljonne, R. H. Friend, *Nat. Chem.* **2013**, *5*, 1019.
[11] M. W. B. Wilson, A. Rao, B. Ehrler, R. H. Friend, *Acc. Chem. Res.* **2013**, *46*, 1330.
[12] C. Ramanan, A. L. Smeigh, J. E. Anthony, T. J. Marks, M. R. Wasielewski, *J. Am. Chem. Soc.* **2012**, *134*, 386.
[13] Y. Wu, K. Liu, H. Liu, Y. Zhang, H. Zhang, J. Yao, H. Fu, *J. Phys. Chem. Lett.* **2014**, *5*, 3451.
[14] M. A. Wolak, J. Delcamp, C. A. Landis, P. A. Lane, J. Anthony, Z. Kafafi, *Adv. Funct. Mater.* **2006**, *16*, 1943.
[15] M. A. Wolak, J. S. Melinger, P. A. Lane, L. C. Palilis, C. A. Landis, J. Delcamp, J. E. Anthony, Z. H. Kafafi, *J. Phys. Chem. B* **2006**, *110*, 7928.
[16] H.-H. Chou, H.-H. Shih, C.-H. Cheng, *J. Mater. Chem.* **2010**, *20*, 798.
[17] Q. Pei, G. Yu, C. Zhang, Y. Yang, A. J. Heeger, *Science* **1995**, *269*, 1086.
[18] L. Edman, *Electrochim. Acta* **2005**, *50*, 3878.
[19] R. D. Costa, E. Ortí, H. J. Bolink, F. Monti, G. Accorsi, N. Armaroli, *Angew. Chem., Int. Ed.* **2012**, *51*, 8178.
[20] Z. Yu, L. Li, H. Gao, Q. Pei, *Sci. China Chem.* **2013**, *56*, 1075.
[21] S. B. Meier, D. Tordera, A. Pertegá, C. Roldán-Carmona, E. Ortí, H. J. Bolink, *Mater. Today* **2014**, *17*, 217.
[22] A. Sandström, A. Asadpoordarvish, J. Enevold, L. Edman, *Adv. Mater.* **2014**, *26*, 4975.
[23] P. Matyba, K. Maturova, M. Kemerink, N. D. Robinson, L. Edman, *Nat. Mater.* **2009**, *8*, 1.
[24] J. D. Slinker, J. A. D. E. Franco, M. J. Jaquith, W. R. Silveira, Y. Zhong, J. M. Moran-Mirabal, H. G. Craighead, H. Ector, D. A. Na, J. A. Marohn, G. G. Malliaras, *Nat. Mater.* **2007**, *6*, 894.
[25] G. G. Malliaras, J. D. Slinker, J. A. DeFranco, M. J. Jaquith, W. R. Silveira, Y.-W. Zhong, J. M. Moran-Mirabal, H. G. Craighead, H. D. Abruña, J. A. Marohn, *Nat. Mater.* **2008**, *7*, 168.
[26] S. Reenen, T. Van Akatsuka, D. Tordera, M. Kemerink, H. J. Bolink, *J. Am. Chem. Soc.* **2013**, *135*, 886.
[27] S. B. Meier, S. van Reenen, B. Lefevre, D. Hartmann, H. J. Bolink, A. Winnacker, W. Sarfert, M. Kemerink, *Adv. Funct. Mater.* **2013**, *23*, 3531.
[28] S. Tang, W.-Y. Tan, X.-H. Zhu, L. Edman, *Chem. Commun.* **2013**, *49*, 4926.
[29] Q. Zhang, B. Li, S. Huang, H. Nomura, H. Tanaka, C. Adachi, *Nat. Photon.* **2014**, *8*, 326.
[30] S. Xue, L. Yao, F. Shen, C. Gu, H. Wu, Y. Ma, *Adv. Funct. Mater.* **2012**, *22*, 1092.
[31] J. Li, T. Nakagawa, J. MacDonald, Q. Zhang, H. Nomura, H. Miyazaki, C. Adachi, *Adv. Mater.* **2013**, *25*, 3319.
[32] L. Duan, J. Qiao, Y. Sun, Y. Qiu, *Adv. Mater.* **2011**, *23*, 1137.
[33] H. Nakanotani, T. Higuchi, T. Furukawa, K. Masui, K. Morimoto, M. Numata, H. Tanaka, Y. Sagara, T. Yasuda, C. Adachi, *Nat. Commun.* **2014**, *5*, 4016.
[34] D. Tordera, J. J. Serrano-Pe, E. Orti, H. J. Bolink, *J. Am. Chem. Soc.* **2013**, *135*, 18008.
[35] P. Coppo, S. G. Yeates, *Adv. Mater.* **2005**, *17*, 3001.
[36] D. Tordera, S. Meier, M. Lenes, R. D. Costa, E. Ortí, W. Sarfert, H. J. Bolink, *Adv. Mater.* **2012**, *24*, 897.
[37] J. C. Scott, G. G. Malliaras, *Conjugated Polymers*, Wiley-VCH, Weinheim, Germany **1999**.
[38] Y. Dong, B. Xu, J. Zhang, X. Tan, L. Wang, J. Chen, H. Lv, S. Wen, B. Li, L. Ye, B. Zou, W. Tian, *Angew. Chem. Int. Ed. Engl.* **2012**, *51*, 10782.
[39] X. Zhang, Z. Chi, B. Xu, L. Jiang, X. Zhou, Y. Zhang, S. Liu, J. Xu, *Chem. Commun.* **2012**, *48*, 10895.
[40] J. U. Engelhart, O. Tverskoy, U. H. F. Bunz, *J. Am. Chem. Soc.* **2014**, *136*, 15166.
[41] C. W. Tang, S. A. Van Slyke, C. H. Chen, *J. Appl. Phys.* **1989**, *65*, 3610.
[42] A. R. Hosseini, C. Y. Koh, J. D. Slinker, S. Flores-Torres, H. D. Abruña, G. G. Malliaras, *Chem. Mater.* **2005**, *17*, 6114.
[43] P. Biegger, S. Stolz, S. N. Intorp, Y. Zhang, J. U. Engelhart, F. Rominger, K. I. Hardcastle, U. Lemmer, X. Qian, M. Hamburger, M. U. H. F. Bunz, *J. Org. Chem.* **2015**, *80*, 582.
[44] J. P. Chen, Y. Okamura, *U.S. Patent 6,962,758*, **2004**.
[45] J. Salbeck, H. Becker, W. Kreuder, K. H. Weinfurtner, *U.S. Patent 6,509,110*, **1999**.
[46] J. E. Anthony, J. S. Brooks, D. L. Eaton, S. R. Parkin, *J. Am. Chem. Soc.* **2001**, *123*, 9482.